Aggregate model of liquids

H. G. Kilian and B. Zink
Abteilung Experimentelle Physik, Universität Ulm, Germany

R. Metzler
Abteilung Experimentelle Physik, Abteilung für Mathematische Physik, Universität Ulm, Germany

(Received 30 April 1997; accepted 13 August 1997)

Atomic-force pictures reveal a heterogeneous microstructure at the surface of glassy layers which should be similar to one of the many equivalent microstructures a liquid is running through. These microstructures are described with the aid of a kinetic model of reversible aggregation which goes back to formulations as used in the description of living polymerization or aggregation of polymers in solution. Aggregates are considered as dynamic subsystems wherein collective modes of motions are excited. Fluctuations of the aggregates, densely packed in a disordered pattern, leads to a broad size distribution which happens to be controlled by Boltzmann's factor. The disordered structure within the aggregates themselves is optimized, reduced aggregate energy and entropy should be equal. Symmetries are deduced which elucidate many universal properties of the dynamic microstructure of liquids. Thermodynamic properties like the specific heats of aggregation in liquids or the dependence of the glass transition of homologues of linear atactic polystyrene are consistently described. [S0021-9606(97)51043-9]

INTRODUCTION

So far, there has been no method of direct detection of the structure of a liquid. Of course, this structure is of a dynamic and disordered nature, varying in time.[1–5] There are results which seem to indicate that this structure is ''heterogeneous'' in space, often studied and debated in the glass transition regime.[6–27] In this situation, atomic-force experiments[28–35] are of importance since they allow us to study the frozen structure at the surface of glassy layers. This structure should be similar to one of the many configurations liquids are running through. Let us recall representative results obtained with these new methods.

Schmidt synthesized so-called ''bottle brush molecules'' [36] a cartoon of which is depicted in Fig. 1. The polystyrene stems grafted on a polymethacrylate chain are atactic and have a mean molecular weight of about $M \sim 40\,000\ \mathrm{g\,mol^{-1}}$. These bottle-brush molecules cannot crystallize.

A Fourier-filtered picture of a monolayer of bottle-brush molecules observed by Sheiko[32] is depicted in Fig. 1. Local orientation of the chains makes the boundaries sharp so that compartments can clearly be identified. The mean diameter of the compartments amounts to about 17 nm. Sheiko[32] studied also the surface on the top of stacks of layers. As shown in Fig. 2, the internal orientation is reduced so that the boundaries of compartments are not as clearly visible as in monolayers. The microstructure of all these layers turns out to be identical, showing a mean diameter of about 15 nm.

Marti *et al.*[28–31] developed a pulsed force scanning mode microscope that allows the scanning of the topography and local adhesion across the surface of glassy layers. A Fourier-filtered picture of a glassy layer of linear polymethylmethacrylate molecules (the surface roughness is below 1 nm!) is depicted in Fig. 3. The mean diameter of the compartments is 21 nm.

For glassy layers of polymethylmethacrylate, the heterogeneous microstructure can be seen better if the surface is wet with ethanole (Fig. 4). Entanglements seem to be concentrated in the interlayers of the microstructure. Swelling of aggregates occur mainly in the direction perpendicular to the surface, by forming humps. The size distribution of the areas is similar to the ones in Figs. 1–3. The mean diameter, slightly increased, is equal to 25 nm.

Above pictures, and others not shown here (anorganic glasses included)[30] reveal, altogether, the same type of microstructure. The mean diameter of the compartments cover a range of 15–30 nm (see below). The size distribution is broad with an asymmetric shape as it is shown in Fig. 5 (see below).

There are some problems which should not be neglected here. With the aid of the above methods compartments smaller than $40-60\ \mathrm{nm}^2$ cannot be identified. This is not a severe restriction since the weight fraction of these entities is small (Fig. 5). A further problem is whether the microstructure at the surface is topologically the same as in bulk. The situation is unique for the monolayers. It is therefore important that the type of microstructures as seen in monolayers, at the surface of stack layers or of glassy sheets with a thickness of some μm is identical. This supports the idea that the microstructure at the surface of a bulky glassy sample should be similar to the one of monolayers.

If above observations are correct, we have to understand them as typical features of liquids and to relate them to the dynamics. In this paper we present a description of the primary elements of the microstructure. Reversible aggregation[37,38] explains the generation of aggregates with a broad size distribution.

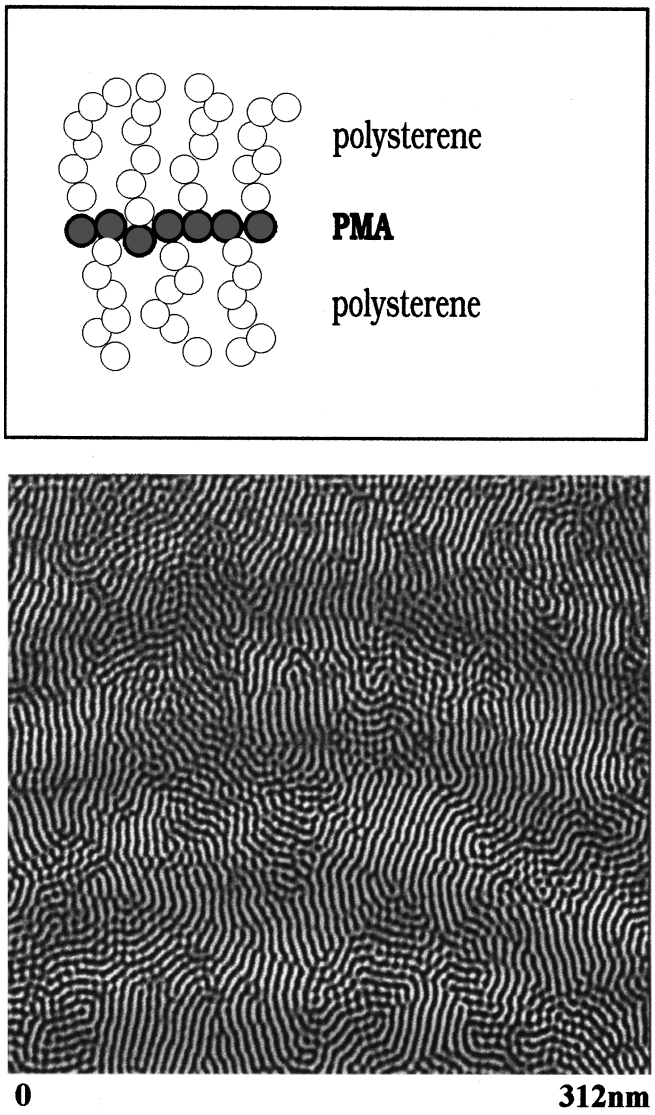

FIG. 1. Fourier-filtered picture of a monolayer of bottle-brush molecules measured in the tapping mode of an atomic force microscope according to Sheiko (Ref. 32). On the top, a cartoon of a bottle-brush molecule with a mean cross-section diameter of about 6 nm. The molecules can directly be seen.

THE KEY PROBLEM

We have to understand why in liquids compact aggregates of different size are generated. Moreover, the intra-aggregate configuration and the whole aggregate ensemble fluctuate.

So far, a theory which explains these phenomena does not seem to exist. Mode-coupling theories[39,40] do not really deal with a dynamics which is related to the microstructure. Jäckle discussed a heterogeneous dynamics in the regime of the glass transition.[23,24] From his model he estimates a dynamical correlation length of about 10 times the mean distance, i.e., about 5 nm. Pechhold[16–18] introduced the meander-model of polymer melts based on the cluster-entropy hypothesis. Yet, meander size distributions like the ones visible in the atomic force pictures, are not yet described. We have presented the conformon model.[41–45] Yet, the size of the conformons is here not defined *a priori*. Moreover, there are objections against the use of the Planck distribution, occurring in this model.

To overcome these and other problems not mentioned here, we introduce the aggregate model of liquids.

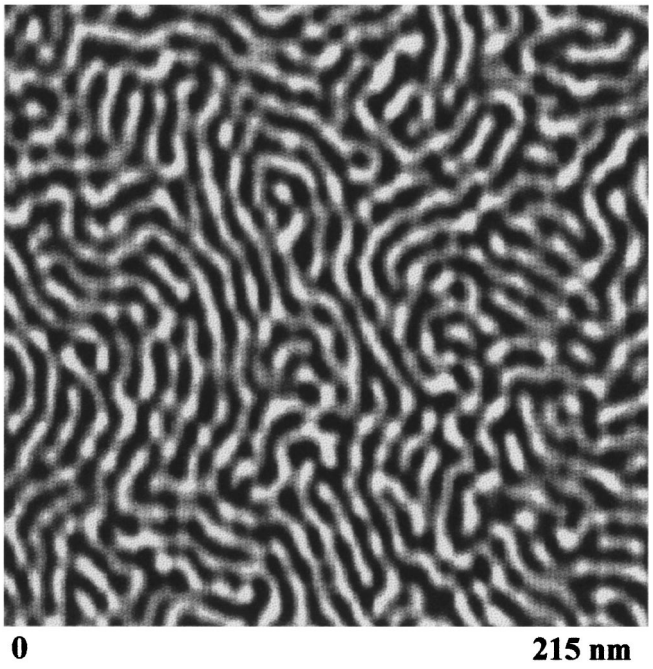

FIG. 2. Fourier-filtered picture of a stack layer of bottle-brush molecules measured in the tapping mode of an atomic force microscope according to Sheiko (Ref. 32).

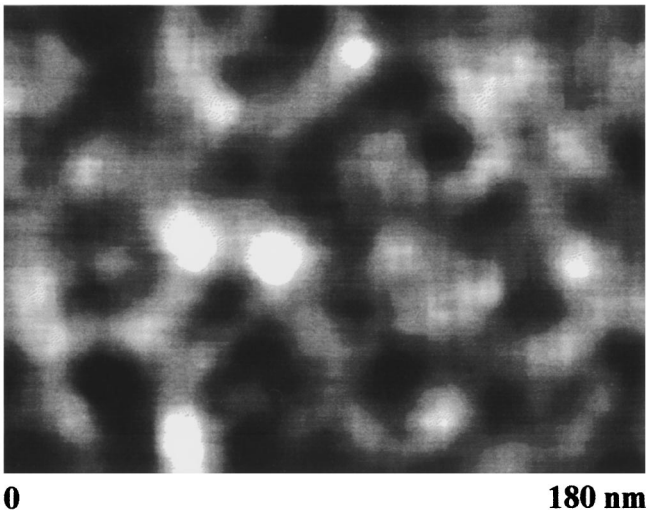

FIG. 3. Fourier-filtered picture of the local adhesion on glassy surface of polymethylmethacrylate (roughness below 1 nm!) measured in the pulsed-force mode of an atomic force microscope according to Zink *et al.* (Ref. 30). The adhesional strength is indicated by different contrasts (brightest areas: Lowest adhesion).

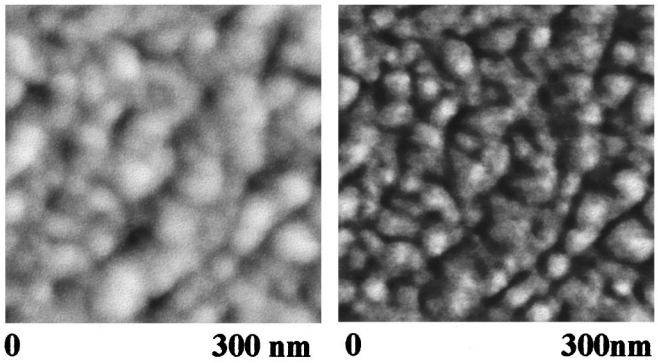

FIG. 4. (A) Topography of on the surface of glassy polymethylmethacrytate layer wetted with ethanol; (B) adhesion pattern of the same sample.

REVERSIBLE AGGREGATION

Let us use the well-known ''void model.'' [4,21,22,46–48] Liquids are described here as binary mixtures comprised of molecules (or molecular segments) and voids. The volume fraction of voids amounts to about 10% ($x_v = 0.1$). Molecules or molecular segments should now ''contact'' next neighbors and generate differently large aggregates with liquidlike internal structures. Aggregation itself should run reversibly. Hence, aggregates have a finite lifetime. Densely packed, the aggregates should constitute typical microstructures like the ones shown in Figs. 1–3. They fluctuate in time, whereby the various configurations should be equivalent in the sense of statistical thermodynamics.

First, we should make suggestions why aggregates exhibit compact configurations. One reason seems to be that the number of contacts of each unit to neighbors is maximized. Since the excess free volume in liquids amounts to about 10%, the mean coordination number within a compact disordered aggregate lies only slightly below the one in a crystal. Compact aggregates are energetically favorable in comparison with linear configurations. It is now difficult to explain why and how the boundaries of the aggregates within the densely packed ensemble are constituted. Defects seem to be squeezed into boundaries, possibly optimizing the intra-aggerate properties. The blobs in Fig. 4 prove an increased concentration of entanglements within boundaries. According to Fig. 1 and 2 fold loops or chain ends seem to be concentrated here. Yet, it remains a future task to identify the origins of these segregation phenomena.

The mean contact energy of units within the compact aggregates is likely to be the same, making the probability of adding another unit to any aggregate identical. The equations developed for describing living polymerization or reversible aggregation[37,48,49] should thus be appropriate for understanding reversible aggregation in liquids. Problems arise for small aggregates. At the moment, we neglect these effects since the number of these aggregates is low (Fig. 5).

According to above assumptions the kinetic equations can be defined by[37,49,50]

$$M_1 + M_1 \leftrightharpoons M_2 : [M_2] = K[M_1]^2,$$

$$M_2 + M_1 \leftrightharpoons M_3 : [M_3] = K[M_2][M_1] = K^2[M_1]^3,$$

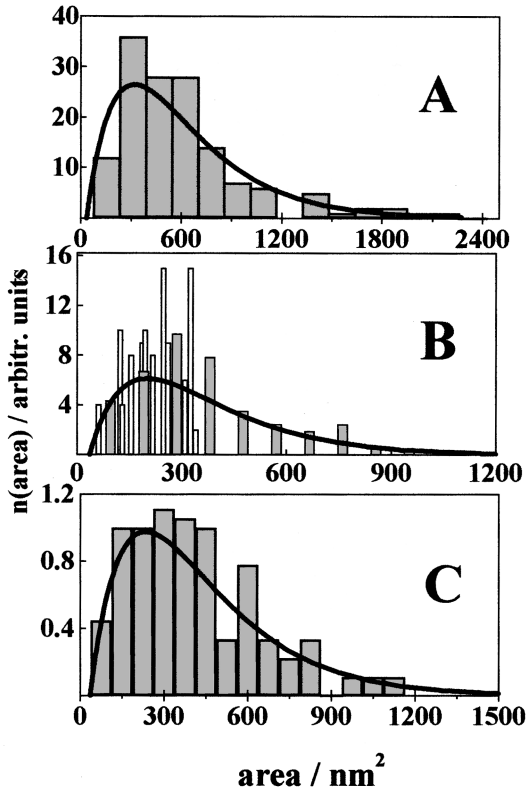

FIG. 5. Histogram of the number distribution of aggregates against the size (area in nm^2): (A) A bottle-brush monolayer (bars) and (B) stack layers of bottle-brush molecules according to Sheiko (Refs. 32). (C) PMMA glassy surface according to Zink *et al.* (Ref. 30). Solid lines are computed with the two-dimensional number distribution $n_2(\text{area}) = h_2(y)/y$ [see Eq. (7)]. Parameters aren collected in Table I.

$$M_{y_0-1} + M_1 \leftrightharpoons M_{y_0} : [M_{y_0}] = K[M_{y_0-1}][M_1] = (K[M_1])^{y_0-1}[M_1]. \quad (1)$$

M_1 is the molecular weight of a single particle; $[M_1]$ is the molar concentration. M_{y_0} is the molecular weight of aggregates consisting of y_0 units; the concentration of these aggregates is written as $[M_{y_0}]$. K is the reaction constant which should not depend on the composition, but may change with temperature. Being identical for all the reactions, K is the only adjustable parameter of the kinetic model. Accounting for the conservation of mass

$$N_0[M_1] \sum_{y_0=1}^{\infty} (K[M_1])^{y_0-1} = 1, \quad (2)$$

with N_0 as normalization constant we are led to the typical Schulz–Flory distribution[37,48–50]

$$n(M_{y_0}) = N_0 \frac{1-x}{[M_1]} x^{y_0-1} : x = K[M_1], \quad (3)$$

$n(M_{y_0})$ is the number of aggregates of a given size y_0, defined as number of units within the aggregate.

TABLE I. Two-dimensional aggregation.

System	x mol^{-1}	$\langle y\rangle$ units[b]	$\langle y\rangle^{1/2}$ $\mathrm{units}^{1/2}$	$\Delta u_{02}/k_BT$
Bottle-brush monolayer	0.9965	333	18.2[a]	0.006
Stack-layer	0.994	250	15.8[b]	0.008
Polymethylmethacrylate	0.995	286	16.9[b]	0.007

[a]Influence of contacts to the substrate.
[b]Within the limits of experimental accuracy identical.

ENERGY-EQUIVALENT AGGREGATES

The shape of aggregates varies as it is recognized from Figs. 1–4. The number of differently shaped isonergetic aggregates should increase with their size. For combinational reasons, this should now be described by the factor $\xi(y)=y^m$. The value of m disposes indirectly the way the equilibrium constant K depends on y. The size distribution of aggregates $h_{m+1}(y)$ as a function of the parameter $y=M_y/M_1$, is then written as

$$h_{m+1}(y)=N_{m+1}\xi(y)y(1-x)x^y=N_{m+1}y^{m+1}(1-x)x^y, \tag{4}$$

with N_{m+1} as normalization constant. If bulk isochoric shapes are equally probable, this entropy-maximum model is characterized by $m=2$. The size distribution $h_3(y)$ is thus equal to

$$h_3(y)=N_3y^3(1-x)x^y. \tag{5}$$

If aggregation at the surface occurs within a few layers, the multipicity should be given by $\xi(y)=y(m=1)$. The two-dimensional size distribution $h_2(y)$ is written accordingly

$$h_2(y)=N_2y^2(1-x)x^y. \tag{6}$$

COMPARISON WITH EXPERIMENTS

The size distribution of the areas of compartments at the surface (Figs. 1–3) is directly deduced from the atomic-force pictures shown above. The data shown in Fig. 5 can be fitted with Eq. (6), by adjusting the only relevant parameter x (besides of the normalization constant N_2). The number distribution is given by $n(\mathrm{area})=h_2(y)/y$. The smallest unit is set to be equal to 36 nm^2. The parameters are collected in Table I.

Large values of x are observed covering a range of $x=0.994$ to $x=0.9965$ (see Table I). K of a liquid with a volume fraction of voids $x_v=0.1$ and $x=0.992$ is equal to [Eq. (3)]

$$K=\frac{x}{[M_1]}=\frac{0.992}{0.9}=1.1044,$$
$$x_{M_1}=0.0082. \tag{7}$$

The small value of x_{M_1} tells us that most of the units should be aggregated. About one percent should be free only. For different values of m the shape of the size distribution is slightly modified. The experimental data can also be reproduced for other values of m so that we cannot unequivocally determine the parameter m. In addition, the absolute value of the parameter y, $y_{\mathrm{abs}}=ys_m$, should be known. Since sufficiently exact molecular details are not available s_m is set equal to 1 nm^3.

Liquids are condensed matter systems where *de facto* all the molecular units are linked in aggregates. The reduced two-dimensional aggregate size distributions of the two different systems studied here, and others not reported, turn out to be similar and nearly identical.[30]

THE STATISTICAL TREATMENT

To develop the statistics of reversible aggregation let us now use, as an approximation, the equilibrium constant for chemical reactions in gases. The equilibrium constant K of the dimerization process is here defined as[38,51]

$$K=e^{-\Delta f_0/k_BT}=\frac{\xi_{M_2}}{\xi_{M_1}^2},$$
$$\xi_{M_1}=\sum_r e^{-u_r(M_1)/k_BT};\quad \xi_{M_2}=\sum_r e^{-u_r(M_2)/k_BT}, \tag{8}$$

with Δf_0 as standard free energy change of dimerization. ξ_{M_k} are the quantum-mechanical partition functions of the molecules involved. $u_r(M_i)$ are the energies of the excited states of the molecule M_i. At equilibrium of dimerization, the condition

$$\Delta f_0=-k_BT\ln\left(\frac{\xi_{M_2}}{\xi_{M_1}^2}\right), \tag{9}$$

must be fulfilled (minimum of the free energy). The expression on the right hand side gives the partial molar entropies of dimerization of the molecules involved.[38] For applying the above model for describing aggregation in liquids one should know the stationary number of modes of motion within the aggregates. Yet, the collective intra-aggregate motions, many of them embracing more than 1000 units, are not known. Analogues to the ξ_{M_k}, therefore, cannot be formulated. By using the ξ_{M_k} symbolically we come, nevertheless, to reliable results.

To deduce now the size distribution of aggregates the probability function x in Eq. (3) is reformulated

$$x=K[M_1]=e^{-(\Delta f_0-k_BT\ln[M_1])/k_BT}. \tag{10}$$

The nominator may be written as

$$\Delta f_0-k_BT\ln[M_1]=\Delta u_0-T\Delta s_0-k_BT\ln[M_1]. \tag{11}$$

Δs_0 is the standard aggregation entropy. We assume now that the partial molar mixing entropy of the units in the non-aggregated liquid $k_B\ln[M_1]$ and Δs_0 are equal, thus

$$\Delta s_0=-k_B\ln[M_1]>0. \tag{12}$$

Δs_0 is then positive. Accordingly, the excess free volume should be scattered across the aggregates in a defined manner, determining their intra-aggregate equilibrium degree of disorder.

With Eqs. (3), (11), and (13) the number distribution of aggregates $n_3(y)$ is deduced to be given by

$$n_3(y) = Cy^2 e^{-y\Delta u_{03}/k_BT} \quad (Cy^m e^{-y\Delta u_{0,m+1}/k_BT}),$$
$$C = \text{const}(1 - e^{-\Delta u_{03}/k_BT}), \tag{13}$$

where Δu_{03} holds for the entropy-maximum model in bulk. For reversible aggregation the Boltzmann factor determines at each temperature their relative fraction. The size distribution of aggregates $h_3(y)$ is then formulated as

$$h_3(y) = Cy^3 e^{-y\Delta u_{03}/k_BT} \quad (Cy^{m+1} e^{-y\Delta u_{0,m+1}/k_BT}). \tag{14}$$

The energy distribution $h_{u3}(y)$ is obtained by multiplying $h_3(y)$ with Δu_{03}

$$h_{u3}(y) = Cy^3 \Delta u_{03} e^{-y\Delta u_{03}/k_BT} \quad (Cy^{m+1} \Delta u_{0,m+1} e^{-y\Delta u_{0,m+1}/k_BT}). \tag{15}$$

The general formulation is shown in brackets.

THE AGGREGATION ENERGY

The crucial parameter is the energy of aggregation, $\Delta u_{0,m+1}$. The volume of liquids increases with temperature. The aggregation energy $\Delta u_{0,m+1}$ should then be positive (see below). Yet, the aggregation contact energy is negative. We should be aware that energy is stored by collective intra-aggregate motions of the ''oscillator type'' which do not occur in the nonaggregated ensemble. If the contact energy is low in comparison with k_BT, $\Delta u_{0,m+1}$ becomes positive if the energy of collective motions is large enough. Our description corresponds to this situation. With the numbers given above we are led to

$$K = 1.104: \quad \xi_{M_2} = 1.104 \xi_{M_1}^2,$$
$$\xi_{M_1} > 1: \quad \xi_{M_2} > \xi_{M_1}^2,$$
$$\frac{\Delta u_0}{k_BT} = \frac{\Delta s_0}{k_B} - \ln K = 0.0064 > 0. \tag{16}$$

Even dimers should exhibit an intrinsic dynamics. This should a *forteriori* hold for large aggregates since the density of collective modes of motion is increased.

THE AGGREGATE ENTROPY

Aggregates as dynamic subunits with a fixed mean energy should also exhibit a defined aggregate-entropy. With the Eqs. (10)–(12), $K = 1.104$ and $[M_1] = 0.9$ we obtain

$$\Delta u_{03} = \Delta f_0 - k_BT \ln[M_1]$$
$$= -k_BT \left(\ln\left(\frac{\xi_{M_2}}{\xi_{M_1}^2} \right) + \ln[M_1] \right)$$
$$= 0.00064 k_BT = k_BT \ln \Omega_0 > 0. \tag{17}$$

The aggregate entropy of a dimer is here characterized by the number of distinguishable configurations Ω_0. Aggregates comprised of y equivalent units are then typified by

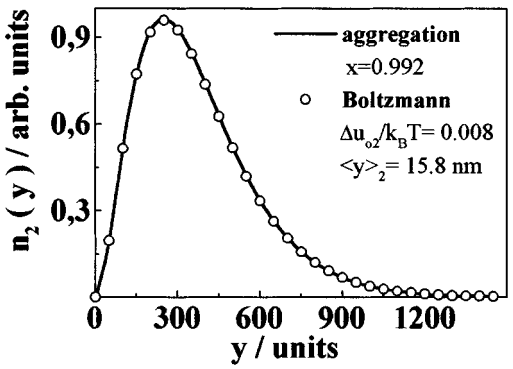

FIG. 6. Number distribution of aggregates plotted against their area: Solid lines: Modified Schulz–Flory distribution of a bottle-brush monolayer [Eq. (5)]; open circles: Boltzmann distribution [Eq. (14)]. We used here $n(\text{area}) = h_2(y)/y$ [Eq. (8)]. The parameters are indicated with the plot and collected in Table II.

$$\frac{y\Delta u_{0,m+1}}{k_BT} = \ln \Omega_y \tag{18}$$

whereby

$$\Omega_y = \Omega_0^y. \tag{19}$$

For $\Delta u_{03}/k_B = 4.2$ K at $T = 300$ K, the dimer shows the small value of $\Omega_0 = 1.014$, corresponding to few distinguishable configurations. For aggregates with 500 units this value grows up to $\Omega_{520} = 1044$ while for aggregates of a size $y = 1000$ one obtains $\Omega_{1000} = 1\,091\,327$.

According to Eq. (18) the aggregation energy $y\Delta u_{0,m+1}$ related to k_BT, should be equal to the reduced entropy $s_y/k_B = \ln \Omega_y$. Aggregates are ''defect saturated'' since the concentration of the excess free volume is locally adjusted accordingly.

COMPARISON WITH EXPERIMENTS

According to Fig. 6 the size distribution of aggregates at the glassy surface can be described, equally well as with eq. (6), by using the two-dimensional formulation of eq. (14) $n_2(y) = h_3(y)/y^2$. One should consider this as proof of the statistical description. The only fitting parameter is the standard aggregation energy Δu_{02}. At $T = 373$ K polymethylmethacrylate shows the ratio $\Delta u_{02}/k_BT = 0.007$. Δu_{02} is substantially smaller than the thermal energy. By the way, the dissociation energy of Na_2[51] at 1000 K is equal to $|\Delta u_0/k_BT| = 0.001\,72$. These numbers explain why a stationary aggregate size distribution should be generated in liquids.

TABLE II. Mean dimensions of PMMA-aggregates for the two- and the three-dimensional model.

Dimension m	$\Delta u_{u,m+1}/k_BT$	$\langle y \rangle$ units	$\langle$Diameter$\rangle$ units
2	0.0061	331	20.5
3	0.0122	246	7.8

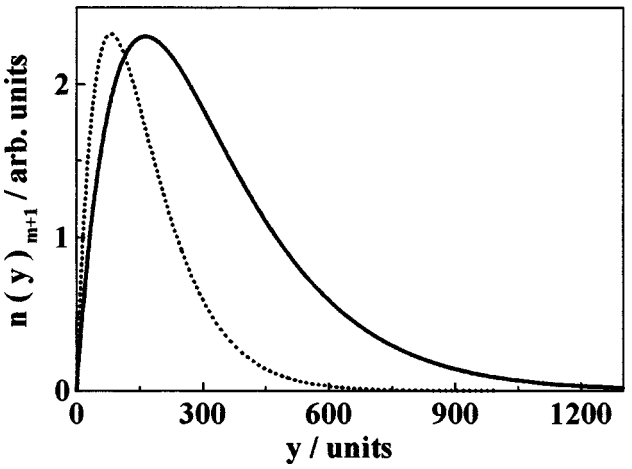

FIG. 7. Aggregate size distribution of the two- and the three-dimensional model;—three-dimensional: $m=2$, $\Delta u_{02}/k_BT=0.0122$;····· two-dimensional: $m=1$, $\Delta u_{03}/k_BT=0.0061$.

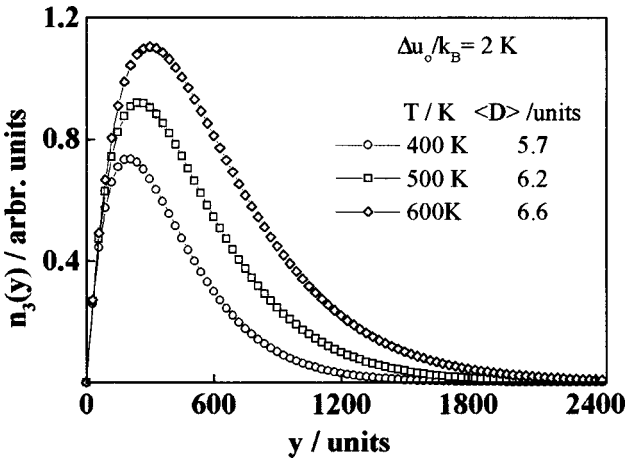

FIG. 8. Number distribution $n_3(y)$ against the aggregate size y computed with $n_3(y)=h_{u3}/y\Delta u_{03}$ [Eq. (16)] at the temperatures as indicated.

THE MICROSTRUCTURE AT THE SURFACE AND IN BULK

In bulk the mean number of aggregation contacts to neighboring molecules, z_3, should be larger than units in a free surface, z_2. With the approximation $z_3=2z_2$, the aggregation energy $\Delta u_{0,m+1}$ is equal to

$$\Delta u_{0,m+1}=(m-1)z_2\Delta u_{02},$$

$$\text{three-dimensional:}\quad m=2:\quad z_3=2z_2. \tag{20}$$

In the bulk the mean size of aggregates should be decreased (Fig. 7) (see below). The mean radius is obtained to amount to $r=(3/4\pi\cdot 214)^{1/3}$ nm$\approx$3.7 nm, i.e., 37 A, fairly comparable with the maximum correlation length deduced from x-ray experiments (about 25 A).[34,35]

According to this simple model the free surface of liquids should exhibit a quasiautonomous dynamics. The reduced coordination number of contacts leads to increased aggregate dimensions. Surface aggregates should have an anisometric shape because of occupying a few layers only.

TEMPERATURE DEPENDENCE OF THE AGGREGATE SIZE DISTRIBUTION

If $\Delta u_{0,m+1}$ is constant, what seems to be a reasonable approximation, the aggregate size distribution is broadened with temperature. This is illustrated in Fig. 8. The mean size of the aggregates

$$\langle y\rangle=\frac{k_BT}{\Delta u_{0,m+1}}\,\frac{\int \eta^{m+1}e^{-\eta}d\eta}{\int \eta^{m}e^{-\eta}d\eta}=(m+1)\,\frac{k_BT}{\Delta u_{0,m+1}}, \tag{22}$$

should increase proportional to the absolute temperature. Since the volume of liquids increases with temperature, the density of aggregates should decrease with their dimensions. This agrees with the finding that the mean adhesion within aggregates seems to decrease with their size.

UNIVERSAL FEATURES

From Eq. (16) we arrive at the reduced energy density distribution

$$h_{ur}=\frac{h_{u3}(\eta_y)}{h_0}=\eta_y^3e^{-\eta_y}\quad(\eta_y^{m+1}e^{-\eta_y}), \tag{23}$$

whereby

$$\eta_y=\frac{y\Delta u_{03}}{k_BT};\quad h_{03}=C\,\frac{(k_BT)^3}{\Delta u_{03}^2}\quad\left(C\,\frac{(k_BT)^{m+1}}{\Delta u_{0,m+1}^m}\right). \tag{24}$$

For a fixed value of m the reduced energy distribution of the aggregate ensemble of liquids is a universal function. Individual properties of molecules in the liquid should not matter. The reduced distribution is predicted to be identical at every temperature. A different formulation of m modifies above relations, yet, the symmetries remain valid. With Eqs. (18) and (23), at the moment not labeling the dimension, we arrive at $(m=2)$

$$h_{ur}(\eta_y)=\frac{\ln^3\Omega_y}{\Omega_y}=h_{sr}(\Omega_y). \tag{25}$$

The reduced energy $h_{ur}(\eta_y)$ and entropy $h_{sr}(\Omega_y)$ of the fraction of aggregates of the type y should be identical. Consequently, the reduced entropy and the reduced energy averaged over the whole aggregate ensemble should also be equal

$$\sum h_{ur}(\eta_y)=\sum h_{sr}\left(\frac{s_y}{k_B}\right)=\Psi, \tag{26}$$

whereby Ψ is a universal constant. This symmetry does not depend on the value, the parameter m is assigned to. The disordered structure of liquids is optimized (minimum free energy).

THERMODYNAMICS

According to the general relations in Eq. (24), the reduced energy $h_{ur}(\eta)$ may be written as

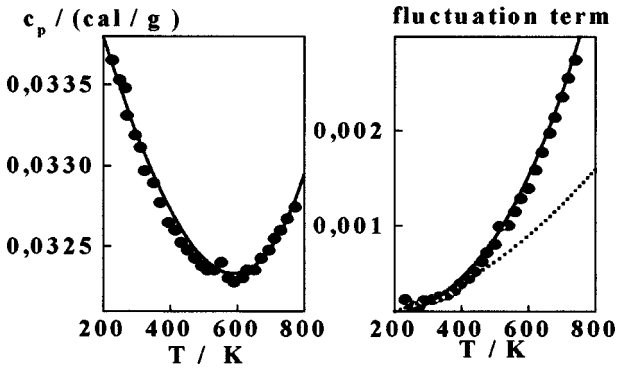

FIG. 9. Specific heats of a mercury melt (●) against the absolute temperature (Refs. 41 and 42). The solid lines are calculated by using Eq. (29) with $c_{po}=a(200\text{-}T)+0.0338$; $a=7.5\ 10^{-6}$ cal/g/K; $b=b=7\ 10^{-12}$ cal/g/K^3; $m=2$. The plot on the right-hand side represents the aggregation term (entropy maximum version); The dotted line belongs the two-dimensional aggregation model ($m=1$).

$$h_{ur}(\eta)=\frac{h_3(\eta)}{\phi_3 k_B^3/\Delta u_0^2}=T^3\eta^3 e^{-\eta},\quad m=2,$$

$$h_{ur}(\eta)_{m+1}=\frac{h_{m+1}(\eta)}{\phi_{m+1}k_B^{m+1}/\Delta u_0^m}=T^{m+1}\eta^{m+1}e^{-\eta},\quad \text{general,} \tag{27}$$

where Φ_3 and Φ_{m+1} are constants. Here, we have also given the general formulations. But, some of the following formulations are only formulated in terms of the maximum entropy model ($m=2$).

Since the front factor is likely to change weakly with temperature, it is not a bad approximation to neglect this effect. By integration the total energy U_{tot} is then obtained to be equal to

$$U_{\text{tot}}=\sigma T^4\int_0^\infty \eta^3 e^{-\eta}d\eta=6\sigma T^4,$$
$$\sigma=\phi_3\frac{k_B^4}{\Delta u_0^3}. \tag{28}$$

The total energy of the aggregate ensemble should increase with temperature, analogously to Boltzmann's law.[38] For a constant front factor and at sufficiently high temperatures, the specific heat capacity of melts $c_p(T)$ should show a typical T^3-dependence superimposed on $c_{p0}(T)$

$$c_p(T)=c_{p0}(T)+bT^3;\quad b=\text{const.} \tag{29}$$

In the Figs. 9 and 10 examples are shown where this dependence is clearly observed.

CONSEQUENCES

The mean reduced energy per aggregate as well as the mean reduced entropy per aggregate should be invariant and given by

$$\langle\eta\rangle=\frac{\int_0^\infty \eta^{m+1}e^{-\eta}d\eta}{\int_0^\infty \eta^m e^{-\eta}d\eta}=\langle s/k_B\rangle=m+1. \tag{30}$$

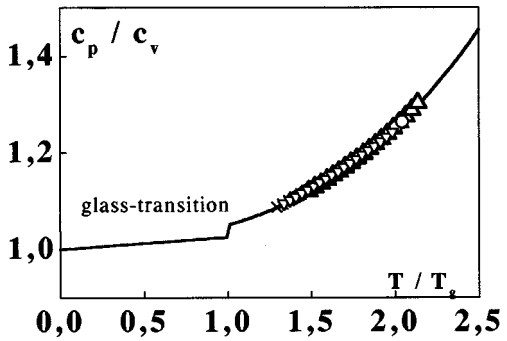

FIG. 10. c_p/c_v of molten n-paraffins melt (○ 11, ◇ $C14$, △ 17; ▽ C 20) against T/T_g (Refs. 41 and 42). Solid lines computed with the aid of an analogue of Eq. (29) (for details see Refs. 41 and 42).

The mean energy is therefore equal to

$$\langle y\Delta u_0\rangle=\langle y\rangle\Delta u_0=(m+1)k_BT. \tag{31}$$

It is reasonable that for $m=2$ the mean energy per aggregate equals a three-dimensional oscillator. With $m=1$ we find the energy of a two-dimensional oscillator.

It is now an interesting consequence of our model that mean intra-aggregate entropy should also be constant

$$\langle s\rangle=(m+1)k_B. \tag{32}$$

For fixed values $m=2$ or $m=1$ the degree of disorder, characterized by the mean reduced aggregate entropy, should be invariant, independent of temperature or of the molecules the liquid is comprised of.

ASYMPTOTICS AT THE GLASS-TRANSITION

A proof of the above predictions is possible by studying the properties of liquids at their glass transition. Idealizing the situation, the transition is taken as a cooperative process with a ''freezing point'' and the above symmetries should also hold just above T_g. With Eq. (18) we arrive at

$$\frac{\langle\Delta u_y\rangle}{T_g}=\frac{\langle y\rangle_g\Delta u_{03}}{T_g}=3k_B=\langle s\rangle_g. \tag{33}$$

Mean energy and entropy of glass formers at the glass-transition temperature related to this temperature should be equal, independent of the molecules the system is comprised of. At T_g the aggregate structure should be identical if we neglect effects due to small differences of the parameter s_m. The correctness of this postulate is proven by the atomic-force measurements which exhibit a nearly identical two-dimensional aggregate structure in systems comprised of so different entities like the bottle-brush-, polymethylmethacrylate-, or polystyrene molecules (not shown here). Moreover, the mean size of the aggregates $\langle y\rangle_g$ of homologues with the same entropy-invariant unit should be identical. This important prediction is checked by describing the glass-transition temperatures of homologues of linear atactic polystyrenes. Since a void is attached to each end of linear chains, (see Figs. 1 and 2) the standard energy of aggregation Δu_{P3} should be reduced in a stoichiometric manner. With the degree of polymerization P this may be expressed by

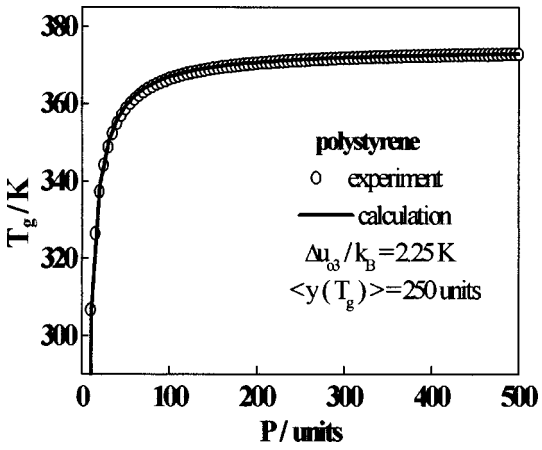

FIG. 11. Quasi-static glass temperatures of linear homologes of atactic polystyrene against the absolute temperature according to Kanig (Refs. 46 and 47). The solid line is computed with the aid of Eq. (35) and the parameters as indicated.

$$\Delta u_{P3} = \Delta u_{\infty 3}\left(1 - \frac{2}{P}\right). \tag{34}$$

Equation (33) is then written as

$$T_g(P) = \langle y\rangle_g \frac{\Delta u_{\infty 3}}{k_B}\left(1 - \frac{2}{P}\right). \tag{35}$$

The quality of the fit to the experimental data of Kanig[46] is seen by evidence from the plot in Fig. 11. In the calculation $\langle y\rangle_g$ constantly equals 250 units. The successful calculation impressively confirms that the aggregate-structure at the glass points of homologues, covering smallest molecules, oligomers, and polymers should in fact be identical.

FINAL REMARKS

Atomic-force experiments reveal the existence of a heterogeneous microstructure at the surface of glassy layers which should be a copy of the many equivalent equilibrium structures at the free surface of a liquid. The aggregate size distributions can be described with the model of reversible aggregation. In bulk the calculated dimensions of the aggregates compare with data deduced from x-ray wide-angle investigations. Hence, the aggregation model yields to relevant parameters of the aggregate structure, at the surface of liquids and in bulk. Representative experiments are fully described, like the ones which prove the thermodynamics of aggregation and like others where relaxation phenomena in different time windows are studied in the linear regime (not shown here[41,43,44]).

According to the aggregate model liquids optimize themselves, by generating a hierarchically organized colloid structure, nonhomogeneous in space. Aggregates are dynamic subsystems with a positive aggregation energy due to the contribution of mode energies. Both, dynamics and structure are strictly related to each other. This seems to hold true within surface layers and in bulk. Universal properties and symmetries of liquids can be recognized, altogether elucidating that energy and entropy of aggregation are always balanced (saturation condition).

It should be mentioned here that the aggregation model allows also to describe the size distribution of clusters formed by carbon blacks (mean size of the primary particles about 60 nm!) or the aggregation of polystyrene vesicles in the liquid state (size of the vesicles in the range of μm!).[52] This underlines the colloid-physical importance of optimization by reversible aggregation.

At the end, let us stress the point that one should understand how the densely packed aggregate ensembles are generated, how their fluctuation is running off. The stationary dynamics in surface layers of liquids should be better defined then it was here. Yet, to accomplish this one needs a well developed physics of global phenomena in densely packed fluctuating ensembles of aggregates with a defined size distribution.

ACKNOWLEDGMENTS

We thank Dr. S. Sheiko for providing the tapping mode pictures of the bottle-brush molecules. We are obliged to Professor Wolfgang Burchard for his kind assistence. We profited from fruitful discussions with Professors Dr. Theo Nonnenmacher, Dr. Hartmut Jex, Dr. O. Marti, Dr. Günter Dukek, Dr. Ingo Asbach, Dr. Gerhard Stoll, and Dr. Joachim Koenen. We are obliged to the DFG (SFB 239) for the generous financial support.

[1] J. Frenkel, edited by L. Voss, *Kinetic of Theory of Liquids* (Leipzig, 1930).
[2] R. B. Bird, O. Hassanger, R. C. Armstrong, and C. F. Curtiss, *Dynamics of Polymeric Liquids* (Wiley, New York, 1977).
[3] D. Richter, A. J. Dianoux, W. Petry, and J. Teixeira, *Dynamics of Disordered Material* (Springer, Berlin, 1989).
[4] N. G. McCrum, B. E. Read, and G. Williams, *Anelastic and Dielectric Effects in Polymeric Solids* (Dover, New York, 1967).
[5] J. D. Ferry, *Viscoelastic Properties in Polymers* (Wiley, New York, 1970).
[6] G. S. Y. Yeh, J. Macromol. Sci. Phys. B **6**, 451 (1972).
[7] G. S. Y. Yeh, J. Macromol. Sci. Phys. B **6**, 465 (1972).
[8] E. W. Fischer, G. Meier, T. Rabenau, A. Patowski, W. Steffen, and W. Tonnes, J. Non-Crystl. Solids **131**, 134 (1991).
[9] P. H. Geil, Ind. Eng. Chem., Prod. Res. Div. **14**, 59 (1975).
[10] G. H. Michler, Acta Polymerica **11**, 709 (1980).
[11] F. Lednicky and Z. Pelzbauer, J. Macromol. Sci. B **21**, 19 (1982).
[12] B. Gerhartz, G. Meier, and E. W. Fischer **92**, 7110 (1990).
[13] St. A. Krivelson, X. Zhao, D. Kivelson, T. M. Fischer, and C. M. Knobler, J. Chem. Phys. **101**, 2391 (1994).
[14] I. Cohen, A. Ha, X. Zhao, M. Lee, T. Fischer, and D. Kivelson (personal communication).
[15] A. Ha, I. Cohen, X. Zhao, M. Lee, and D. Kivelson, J. Phys. Chem. **100**, 1 (1996).
[16] W. Pechhold, M. Böhm, and W. v. Soden, Progr. Coll. Polym. Sci. **75**, 23 (1987).
[17] W. Pechhold, O. Grassl, and W. v. Soden, *Crosslinking and Scission in Polymers*, edited by O. Güven (Kluwer, Dordrecht, 1990), p. 199.
[18] W. Pechhold, *Crosslinking and Scission in Polymers*, edited by O. Güven (Kluwer, Dordrecht, 1990), p. 223.
[19] G. H. Michler, *Kunststoff-Mikromechanik*, edited by Carl Hanser (München-Wien, 1992).
[20] J. H. Gibbs, *Modern Aspects of the Vitreous State, Vol I*, edited by J. D. Mackenzie (Butterworth, London, 1964).
[21] A. J. Kovacs, Fortschr. Polymer Forsch. **3**, 394 (1963).

[22] R. N. Haward, *The Physics of Glassy Polymers* (Appl. Sci. Publ. LTD, London, 1973).
[23] J. Jäckle, Rep. Progr. Phys. **49**, 171 (1986).
[24] J. Jäckle, Phys B1. **52**, 351 (1996).
[25] G. Kanig, Koll. Z. Z. Polym. **233**, 829 (1957).
[26] R. V. Chamberlin and D. W. Kingsbury, J. Non-Cryst. Solids **172**, 318 (1994).
[27] M. L. Williams, R. F. Landel, and J. D. Ferry, J. Am. Chem. Soc. **77**, 3701 (1955).
[28] O. Marti, Surface and Coatings Techn. **62**, 510 (1993).
[29] O. Marti and J. Colchero, Phys B1. 48, **12**, 1007 (1992).
[30] B. Zink, H. G. Kilian, O. Marti, and H. Hild (to be published).
[31] M. Hipp, B. Bielefeldt, J. Colchero, and O. Marti, J. Mlynek **42**, 1498 (1992).
[32] S. Sheiko (to be published).
[33] H. G. Kilian, Macromol. Chem., Macromol. Symp. (in press).
[34] B. Steffen, R. Hosemann, Phys. Rev. B. **13**, 3232 (1976).
[35] B. Steffen, Phys. Rev. B **13**, 3227 (1976).
[36] W. Wintermantel and M. Schmidt., Macromol. Chem., Rapid Comm. **15**, 279 (1994).
[37] W. Burchard, Advances of Coll. Interface Sci. **64**, 45 (1996).
[38] F. Reif, *Statistical and Thermal Physics*, Internat. Student Ed. (McGraw-Hill, Cogakusha LTD, Tokyo, 1965).
[39] W. Götze and L. Sjoergren, Rep. Progr. Phys. **55**, 241 (1992).
[40] K. L. Ngai, Commun. Solid State Phys. **9**, 127 (1979).
[41] H. G. Kilian, Physica Scipta **55**, 219 (1994).
[42] H. G. Kilian, C. Beyer, and M. Pietralla, Macromol. Chem., Macromol. Symp. **90**, 1 (1995).
[43] H. G. Kilian, Coll. Polym. Sci. **273**, 828 (1995).
[44] H. G. Kilian and W. Glöckle, Polymerica Acta **47**, 150 (1996).
[45] H. G. Kilian, Macromol. Symp. **113**, 81 (1997).
[46] G. Kanig, Kolloid Z. Z. Polym. **190**, 1 (1963).
[47] G. Kanig, Kolloid Z. Z. Polymere **233**, 831 (1969).
[48] H. G. Kilian, Colloid Polym. Sci. **252**, 353 (1974).
[49] R. C. Schulz, Z. Physikalische Chemie B**43**, 25 (1939).
[50] H. G. Elias, *Makromoleküle* (Hüthig&Wepf-Verlag, Basel-Heideberg, 1971).
[51] W. J. Moore and D. O. Hummel, *Physikalische Chemie* (deGruyter, Berlin-New York, 1973).
[52] J. N. Israelachvili, Intermolecular and Surface Force, 2nd. ed. (Academic New York, 1992).